Available online at www.sciencedirect.com
ScienceDirect
Catalysis Today 137 (2008) 267–272
CATALYSIS TODAY
www.elsevier.com/locate/cattod

Kinetic investigation of the NO decomposition over V–O–W/Ti(Sn)O_2 catalyst

J. Banaś [a], M. Najbar [a], V. Tomašić [b,*]

[a] *Department of Chemistry, Jagiellonian University, Ingardena 3, Cracow, Poland*
[b] *Faculty of Chemical Engineering and Technology, University of Zagreb, Marulićev trg 19, 10000 Zagreb, Croatia*

Available online 12 February 2008

Abstract

A kinetic study of the NO decomposition over V–O–W/Ti(Sn)O_2 catalyst carried out in a tubular fixed-bed reactor operating under atmospheric pressure at different temperatures and at various space times is presented. Assuming that NO decomposition occurs as a result of electron transfer from the metal active site to antibonding π NO orbital, several kinetic models were derived and applied to describe the kinetics of reaction. The best agreement between the experimental data and theoretical prediction was achieved with the model assuming adsorption of NO on the active sites as the rate-determining step. Finally, it was concluded that V–O–W/Ti(Sn)O_2 catalyst has promising activity for the NO removal in O_2 presence from the effluent gases of the different sources of emission.

Keywords: Kinetics of NO decomposition; V–O–W/Ti(Sn)O_2 catalyst

1. Introduction

Nitrogen oxides (NO_x) are hazardous air pollutants. Concern for environmental and health issues coupled with stringent NO_x emission standards generates a need for the development of efficient low-cost NO_x abatement technologies. The emission abatement of NO_x may be achieved by the combustion modifications by the flue gas post-treatments, such as selective catalytic reduction (SCR), selective non-catalytic reduction (SNCR), adsorption, scrubbing and biological degradation [1–3].

It is known that nitrogen monoxide (NO) is the dominating NO_x component in the flue gases. The direct decomposition of NO over appropriate catalysts is still the most attractive catalytic method for NO_x emission abatement. Unfortunately, the best catalysts for this reaction (e.g. copper-exchanged ZSM zeolites) are currently not stable enough under high-temperature reaction conditions to be applied practically [4]. On the other hand, the most frequently used commercial SCR catalysts containing V_2O_5 and WO_3 and/or MoO_3 show relatively stable activity in NO decomposition [5–7]. A summary of the results of kinetic studies on NO decomposition reported by different investigators and obtained under various reaction conditions is shown in Table 1. It has been discovered that regardless the catalyst used, one of the most important problems is inhibition of NO decomposition by oxygen which is produced by the reaction or is present in the feed stream [8].

This work reports on kinetics of NO decomposition over nanostructured V–O–W/Ti(Sn)O_2 catalyst. The ability of the V–O–W/Ti(Sn)O_2 to catalyze the reduction of nitric oxide to nitrogen is related to the surface structure of the catalyst. Special attention is given to the activation of the reduced catalyst by the oxygen formed in NO decomposition. The surface reconstruction resulting in the catalyst activation is discussed. Comparison of V–O–W/Ti(Sn)O_2 with Cu/ZSM-5 zeolite was also made and some conclusions about potential catalyst for the NO decomposition are drawn.

2. Experimental

2.1. Preparation of the rutile supported nanostructured V–O–W catalyst

Ti(Sn)O_2 support as well as a Ti(Sn)O_2-supported vanadia-tungsta catalyst were obtained using sol–gel method [17]. Titanium isopropoxide (Aldrich, 97%) was diluted in iso-

* Corresponding author. Tel.: +385 1 4597 281; fax: +385 1 4597 260.
E-mail address: vtomas@fkit.hr (V. Tomašić).

0920-5861/$ – see front matter © 2008 Elsevier B.V. All rights reserved.
doi:10.1016/j.cattod.2007.12.116

Nomenclature

C_{NO}, C_{O_2}	concentration of indicated compound (mol dm^{-3})
d_p	mean pore diameter (nm)
k	rate constant
K	number of measurements performed at different temperatures
K_A	adsorption equilibrium constant for NO (dm^3 mol^{-1})
K'_D	adsorption equilibrium constant for oxygen (dm^3 mol^{-1})
M	number of estimated parameters
n	reaction order with respect to NO
N	number of data points
r_A	reaction rate mol (dm^{-3} s^{-1})
r_S	surface reaction rate (mol dm^{-3} s^{-1})
S	specific surface area (m^2 g^{-1})
SD	normalized square deviation
$\overline{SD}$	mean square deviation
T	temperature (K)
V_p	total pore volume (cm^3 g^{-1})
y_i	molar fraction of compound i
y_{NO}, y_{NO_2}	molar fraction of indicated compound
y_{exp}	experimentally obtained results
Y_{th}	theoretically obtained results

Greek letters

τ	reactor space time (s)
τ/τ_{max}	normalized reactor space time

propanol (Aldrich, 99.5%) at room temperature and next nitrogen flew through the obtained mixture to avoid its hydrolysis. Then tin chloride (Aldrich, 99.95%) was added (Ti:Sn = 80.2:19.8 of atomic ratio). The mixture of titanium and tin isopropoxides was added by drop to water with the small amounts of isopropanol at continuous stirring. Obtained sol was heated to 80 °C, and then this temperature was maintained up to solvent evaporating. Xerogel was dried and calcined at 460 °C in air for 3 h. Ti(Sn)O_2 support was grinded in an agate mortar and then added to water heated to 80 °C and continuously stirred for 1 h.

Tungsten chloride (Aldrich, 99.9 %) was diluted in isopropanol with the proper amount of vanadyl isopropoxide (Johnson Matthey, 95–99%) to obtain V:W = 1:9 of atomic ratio. The mixture of isopropoxides was stirred and heated to 80 °C. This temperature was retained for 1 h. Then the mixture was added to the sol solution of the support and the obtained gel was stirred at 80 °C up to solvent evaporation. Obtained catalyst precursor was dried and calcined at 460 °C in air for 3 h.

2.2. Preparation of the Cu-containing pentasil zeolite

Na/ZSM-5 with Si/Al molar ration of 54 was supplied by Leuna Werke. The Cu-containing pentasil zeolite (Cu/ZSM-5) was prepared by ion exchange of Na/ZSM-5 (10 g) with 0.01 mol dm^{-3} of aqueous solution of copper(II) acetate (1 dm^3). Ion exchange was performed overnight at room temperature. Copper content was 1.99 wt.%. The obtained catalyst was washed, filtered and dried overnight at 373 K. The zeolite powder was pressed into tablets, crushed and sieved. The pretreatment of the catalysts at 400 °C in helium flow (40 cm^3 min^{-1}) for 1 h was performed before catalytic reaction.

2.3. Catalyst characterization

The prepared catalysts were characterized by several techniques, such as XRD, surface measurements and thermal analysis (DSC/TG). Textural characterization of the monolith samples was performed by means of nitrogen adsorption/desorption isotherms at −196 °C using Micromeritics ASAP 2000 instrument. The physical properties of both catalysts, such as specific surface area, total pore volume and mean pore diameter are given in Table 2. Detailed characterization of surface species structures of the V–O–W/Ti(Sn)O_2 catalyst obtained by Raman spectroscopy is presented elsewhere [6].

2.4. Experimental apparatus and procedures

The catalytic properties of a V–O–W/Ti(Sn)O_2 (r) catalyst and metal containing ZSM-5 were investigated at the temperature range from 165 to 500 °C and at atmospheric

Table 1
The results of former kinetics studies on NO decomposition

Investigator	Catalyst type	Reaction conditions	Reaction order with respect to NO	References
Sakaida et al.	Ni-Pt/Al_2O_3	T: 427–538 °C; 1–15 atm; 0.4% NO/N_2	2	[9]
Amirnazmi et al.	Pt/Al_2O_3	T: 600–1000 °C; 1 atm; 1–10% NO/He, 1–7% O_2/He	1	[10]
Iwamoto et al.	CuY	T: 300–550 °C; 1 atm; 4% NO/He	1.6	[11]
Li and Hall	CuZSM-5 (Si/Al = 26)	T: 350–550 °C; 1–4% NO/He, 0.5–1% O_2/He	1-1.2	[8]
Teraoka et al.	$La_{0.8}Sr_{0.2}CoO_3$; $La_{0.4}Sr_{0.6}Mn_{0.8}Ni_{0.2}O_3$	T: 500–800 °C; 1 atm; 0.1–1% NO/He, 0–9% O_2/He	2	[12]
Campa et al.	CuY; CuZSM-5	T: 500 °C; 1–14% NO/He	1.5–1.8; 1.1–1.3	[13]
Vannice et al.	La_2O_3; Sr/La_2O_3	T: 650 °C; 1 atm; 0.4–1.8% NO/He, 0–1% O_2	1.22–1.46; 1.08–1.11	[14]
Haneda et al.	Co_3O_4	T: 450–600 °C; 1 atm; 0.5–3.% NO/He, 0–5% O_2	1.21–1.47	[15]
Zhu et al.	$La_{0.4}Sr_{0.6}Mn_{0.8}Ni_{0.2}O_3$	T: 500–850 °C; 1 atm; 0.5–2.0% NO/He	∼1	[16]

Table 2
Physical properties of the catalysts

Catalyst	S ($m^2\ g^{-1}$)	V_p ($cm^3\ g^{-1}$)	d_p (nm)
V–O–W/Ti(Sn)O_2	66.73[a]	0.1560	9.3826
Cu/ZSM-5	355.6208[b]	0.1520	1.7095

[a] By BET method.
[b] By Langmuir model.

pressure. A 0.315–0.5 mm-size fraction was used for the catalytic tests.

Steady-state NO decomposition rates were measured using a tubular fixed-bed reactor (6.5 mm i.d. and 150 mm length) with the catalyst samples supported on a porous quartz frit. Reaction was performed at atmospheric pressure and at various reactor space times. Space times were changed by varying total flow rate of the reactant gas (4% NO in helium; Messer Griesheim) over constant mass of the catalyst (0.5 g). The catalyst activity for NO decomposition was evaluated by conversion of NO into N_2. The reactor effluent was analyzed combining volumetry and gas chromatography (GC). The procedure was performed firstly by the removal and volumetric analysis of NO_2 using Saltzman technique. Traces of H_2O were removed by passing the effluent through a $CaCl_2$ bed. The gaseous products N_2, O_2, and NO were analyzed by GC (Varian 3300) equipped with a TCD detector using a stainless steel column packed with a molecular sieve 5A (80/100 mesh). Helium was used as carrier gas. A complete description of experimental apparatus and procedures can be found elsewhere [18].

3. Discussion and results

The DSC curves and mass losses obtained for Cu/ZSM-5 and V–O–W/Ti(Sn)O_2 (r) catalyst are shown in Fig. 1a and b. Endothermic peaks appearing at the beginning of DSC curves (at 74.3 °C and 54.4 °C for Cu/ZSM-5 and V–O–W/Ti(Sn)O_2, respectively) correspond to the loss of water and volatile compound from the catalyst samples. The first exothermic peak on DSC Cu/ZSM-5 curve (297.5 °C) can be attributed to the copper oxidation and the second one (1135.1 °C) to the zeolite recrystallisation. The increase of the mass of V–O–W/Ti(Sn)O_2 catalyst at 300–1100 °C might be ascribed to the oxidation of the vanadium segregating on the surface of the V–W oxide bronze crystallites as vanadia-like species [19]. On DSC curve vanadium oxidation is demonstrated as a very large exothermic peak. The additional DSC peak at 748.9 °C shows that vanadium segregation is followed by orthorhombic–tetragonal WO_3 transformation observed by Roth and Waring [20].

Fig. 2a illustrates the change in the molar fraction of the reaction products over V–O–W/Ti(Sn)O_2 (r) catalyst as a function of space times at temperature of 165 °C. It can be seen that molar fraction of the nitrogen and oxygen at the reactor exit are almost the same, indicating that secondary reaction between the unreacted NO and oxygen produced by main reaction was not favourable under the conditions employed in this study. As it is well known, the oxidation of NO into NO_2 is scarce example of the oxidation reaction with the rate increasing with decrease of the reaction temperature and is favourable at room

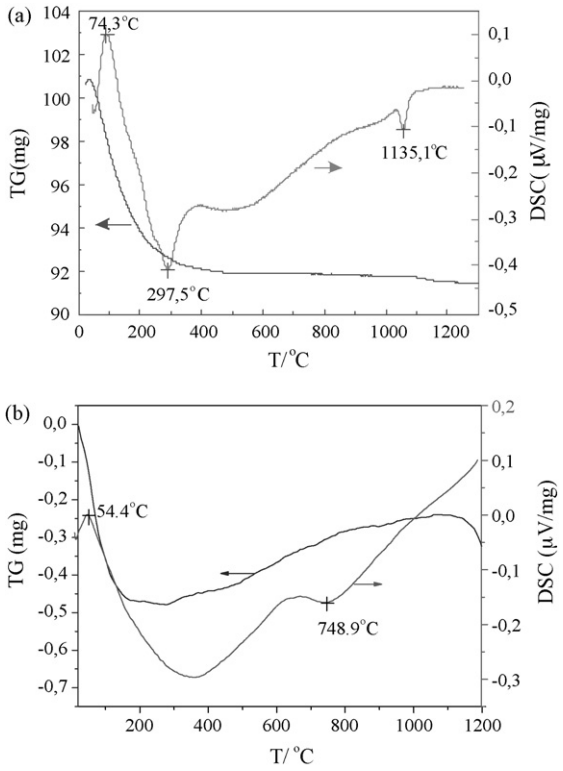

Fig. 1. Results of the TG/DSC analysis of (a) Cu/ZSM-5 and (b) V–O–W/Ti(Sn)O_2 (r) catalyst.

temperature. This is confirmed by the results given in Fig. 2b, indicating that secondary reaction presumably takes place in the cold part of the reaction system [18].

As already mentioned, this work was aimed at the investigation of the kinetics of NO decomposition over V–O–W/Ti(Sn)O_2 catalyst. Taking into account the sequence of elementary steps in the overall reaction mechanism and assuming that one of those steps was the slowest one (or rate-determining step, rds) several rate equations were derived. The survey of the kinetic models used in the present study is given in Table 3. The empirical power-low model was tested too. As was shown earlier [21] NO is adsorbed on metal atoms in vanadia-like surface species via nitrogen atom (ON-Me). Thus the mechanism (2) and (3) in Table 3 should first of all be taken into account.

Experimental values for the reaction rate were obtained according to the model for tubular reactor:

$$-\frac{dy_{NO}}{d\tau} = f(y_i) \quad (5)$$

Mathematical model for the tubular reactor (Eq. (5)) was developed under the following assumptions: steady state and isothermal conditions, ideal gas flow and neglected pressure drop through the catalytic layer. Values of the space times were normalized by dividing with maximum value (τ_{max}) in order to compare the mean square deviations obtained at different measurements.

Differential equations obtained by inserting the proposed kinetic models into the reactor model (Eq. (5)) were solved

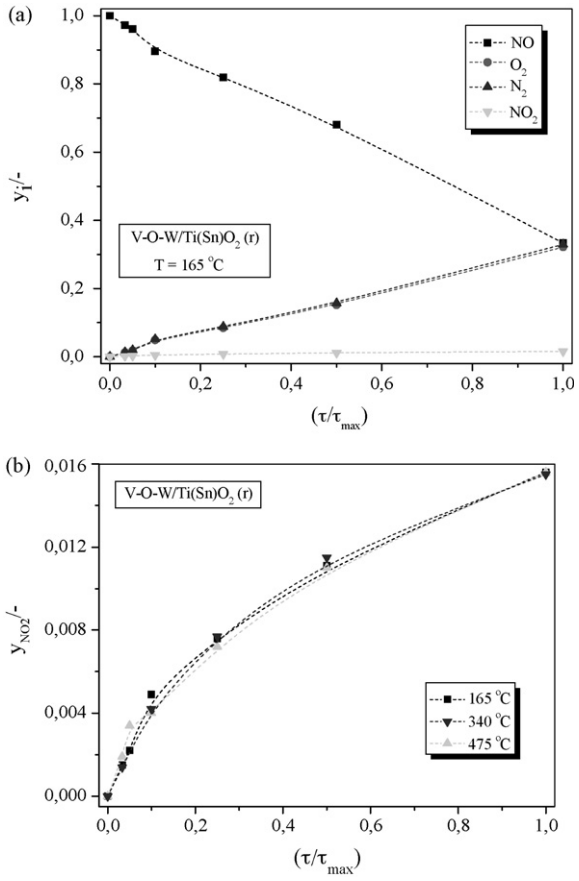

Fig. 2. Change in the molar fraction of the reaction products over V–O–W/Ti(Sn)O_2 (*r*) catalyst as a function of space times at temperature of 165 °C (a). Influence of the space times and reaction temperature on the molar fraction of NO_2 at the exit from the reactor (b).

numerically by the 4th order Runge–Kutta algorithm under simultaneous assessment of the kinetic parameters (Nelder–Mead method of nonlinear regression). The selection of a suitable model was based on minimization of the squares of differences between experimentally obtained ($Y_{exp.}$) and predicted results ($Y_{th.}$).

$$SD = \frac{1}{N-M}\sqrt{\sum_{i=1}^{N}(Y_{exp.} - Y_{th.})^2} \quad (6)$$

The obtained kinetic parameters and the appropriate mean square deviations are summarised in Table 4. The mean value of the square deviations obtained at different temperatures was calculated using the following expression:

$$\overline{SD} = \frac{\sum_{i=1}^{K} SD}{K} \quad (7)$$

As shown in Table 4 and Fig. 3a, the best fit to the experimental data was achieved using the simple power-low model (mean SD = 2.111×10^{-2}). However, this model has no practical importance and it can be used only as fast screening technique in discovery and study of various catalysts for the desired purpose. Thus, experimental data were correlated with several mechanistic Langmuir–Hinshelwoods (LH) models. The differences among them were in the type of interactions between the reactants and active sites on the catalyst surface, in the assumed oxygen (or nitrogen) desorption from the active sites, as well as in the number of reaction parameters. The LH models given by Eq. (2), and Eq. (3) had two parameters, while model given by Eq. (4) had three parameters. Satisfactory degree of correlation was established, especially by using LH kinetic model given by Eq. (2). This model was developed assuming NO adsorption as the rate-determining step. These results are in good agreement with the observation of Li and Hall [8] who used similar model to describe NO decomposition over Cu/ZSM-5 catalyst. As can be seen from the values of the mean square deviations, the other two LH models also agree well with the experimentally obtained results. However, it is important to emphasise that kinetic data cannot be used to determine which reaction mechanism is correct. Apparently, additional experimental work is necessary to validate proposed kinetic model. According to the literature, formation of the

Table 3
The kinetic models proposed in present study

Empirical model

$r_A = kC_{NO}^n$	(1)

Mechanistic models

Reaction mechanism	Rate equation	
NO + S → S·NO (rds); 2S·NO → O_2 + 2S·N; 2S·N ↔ N_2 + 2S	$r_A = \frac{k \cdot C_{NO}}{1+\sqrt{K'_D \cdot C_{N_2}}}$	(2)
NO + S ↔ S·NO; 2S·NO → O_2 + 2S·N (rds); 2S·N ↔ N_2 + 2S	$r_S = \frac{k \cdot C_{NO}^2}{\left(1+\sqrt{K'_D \cdot C_{N_2}}\right)^2}$	(3)
NO + S ↔ S·NO; 2S·NO → O_2 + S·N_2 + S (rds); S·N_2 ↔ N_2 + S	$r_S = \frac{k \cdot C_{NO}^2}{(1+K_A C_{NO}+K'_D \cdot C_{N_2})^2}$	(4)

Table 4
Kinetic parameters of NO decomposition over V–O–W/Ti(Sn)O_2 (*r*) catalyst and the mean square deviations

	T (°C)				
	165	340	400	420	475
Model 1 (Eq. (1))					
k ($\times 10^{-2}$ (mol dm^{-3})$^{1/n-1}$ s^{-1})	3.738	3.737	6.046	4.158	3.864
n ($\times 10^2$)	20.710	21.470	0.024	0.280	20.960
SD ($\times 10^2$)	1.519	1.352	5.540	0.888	1.254
Mean SD ($\times 10^2$)			2.111		
Model 2 (Eq. (2))					
k ($\times 10^{-2}$ s^{-1})	5.735	5.738	1.117	6.252	6.282
K'_D ($\times 10^{-2}$ dm^3 mol^{-1})	0.013	0.024	0.015	2.464	2.490
SD ($\times 10^2$)	2.625	1.974	4.499	2.755	3.726
Mean SD ($\times 10^2$)			3.116		
Model 3 (Eq. (3))					
k ($\times 10^{-5}$ dm^3 mol^{-1} s^{-1})	4.754	4.803	10.070	4.908	4.887
K'_D (dm^3 mol^{-1})	2.797	2.730	2.147	1.599	2.853
SD ($\times 10^2$)	4.354	3.916	7.865	4.502	5.419
Mean SD ($\times 10^2$)			5.209		
Model 4 (Eq. (4))					
k ($\times 10^{-5}$ dm^3 mol^{-1} s^{-1})	5.949	5.994	11.580	6.160	6.073
K_A ($\times 10^{-2}$ dm^3 mol^{-1})	1.048	1.039	0.086	1.028	1.035
K'_D ($\times 10^{-2}$ dm^3 mol^{-1})	1.032	1.032	0.086	1.023	1.025
SD ($\times 10^2$)	4.044	3.582	7.327	4.193	5.109
Mean SD ($\times 10^2$)			4.851		

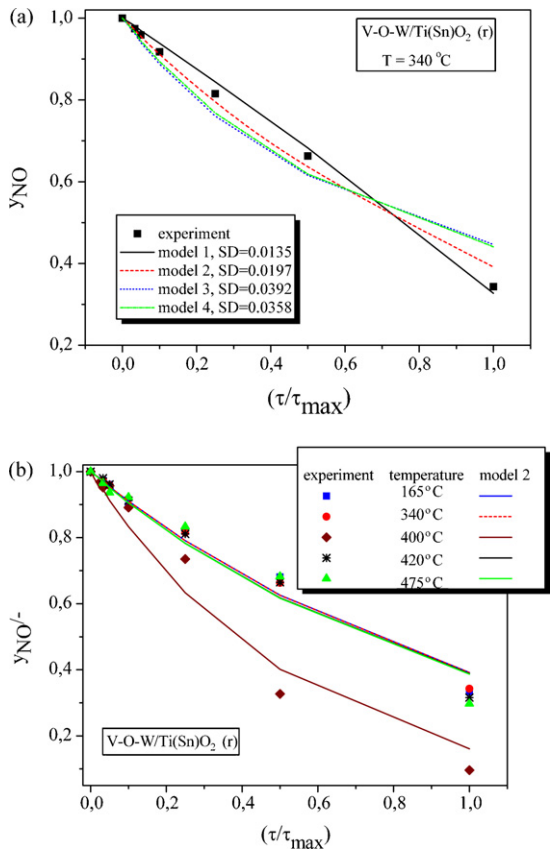

Fig. 3. Comparison of the experimental data (points) and theoretical predictions: (a) obtained by different models (as indicated in Table 3) and (b) obtained over V–O–W/Ti(Sn)O_2 (*r*) by model given by Eq. (2).

reaction intermediates such as N_2O, NO_2 or NO_2^- could be the key step for NO decomposition [22]. The formation of such reaction intermediates during NO decomposition over V–O–W/Ti(Sn)O_2 catalyst is really observed [23].

The influence of the reaction temperature on the molar fraction of NO at the exit from the reactor is shown in Fig. 3b. The results show that NO decomposition proceeds with the reasonably high conversion over V–O–W/Ti(Sn)O_2 catalyst at the temperature of 400 °C (conversion of 84% at τ_{max}), while conversions obtained at other temperatures are ca. 26% lower.

Comparison of the activity of V–O–W/Ti(Sn)O_2 and Cu/ZSM-5 catalyst in NO decomposition is illustrated in Fig. 4. Despite the fact that the specific surface area of Cu/ZSM-5

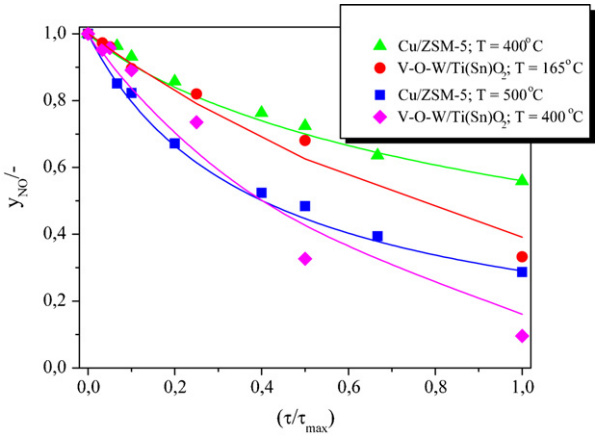

Fig. 4. The molar fraction of the unreacted NO in the reaction products as a function of the catalyst type and reaction temperature. Kinetic parameters are given in Table 4.

catalyst yields 355.62 $m^2\ g^{-1}$ and specific surface area of V–O–W/Ti(Sn)O_2 catalyst is much smaller (66.73 $m^2\ g^{-1}$), the latter catalyst shows better activity at 400 °C. The highest activity of Cu/ZSM-5 is obtained at 500 °C, but this activity is still smaller than activity of V–O–W/Ti(Sn)O_2. Moreover, V–O–W/Ti(Sn)O_2 catalyst shows high activity even at temperature of 165 °C, which is of great importance for its practical applications in the real conditions. In our other paper [6] it has been observed that oxygen produced by NO decomposition, especially at higher space times in the reactor leads to the rate enhancement. This is attributed to the reconstruction of the catalyst surface due to vanadium segregation and oxidation (see Fig. 1b) by the oxygen formed in NO decomposition. As it was shown earlier [6] the oxygen interaction with the reduced catalyst surface causes oxidation of the vanadium atoms segregated on V–O–W bronze crystallites, resulting in the formation of the vanadia-like monolayer species. These species show high activity in NO decomposition. This beneficial influence of the oxygen on the catalyst activity in NO decomposition to N_2 and O_2 is, according to our knowledge, observed for the first time.

4. Conclusions

In this study the V–O–W/Ti(Sn)O_2 (*r*) was used as catalyst for NO decomposition. The V–O–W/Ti(Sn)O_2 catalyst, which was prepared by a sol–gel method, exhibited the enhanced catalytic properties in comparison to the metal containing ZSM-5 zeolite, especially at lower reaction temperatures. It is found out that the rate of NO decomposition over V–O–W/Ti(Sn)O_2 catalyst can be described with the LH type of reaction mechanism, assuming that the NO adsorption is the rate-determining step of the process. Finally, it has been concluded that V–O–W/Ti(Sn)O_2 catalyst has promising activity for the NO removal from the exhaust streams.

Acknowledgements

M. Najbar and J. Banas thank the Committee of Scientific Research, Grant BPZ-KBN-116/T09/2004 for the financial support. V. Tomašić highly appreciates financial support of the Croatian Ministry of Science, Education and Sport.

References

[1] H. Brauer, Y.B.G. Varma, Air Pollution Control Equipment, Springer-Verlag, Berlin, 1981.
[2] N.N. de Nevers, Air Pollution Control Engineering, McGraw-Hill, New York, 1995.
[3] C.D. Cooper, F.C. Alley, Air Pollution Control—A Design Approach, Waveland Press Inc., Long Grove, 2002.
[4] J.N. Armor, Catal. Today 26 (1995) 99.
[5] M. Najbar, J. Banaś, J. Korchowiec, A. Białas, Catal. Today 73 (2002) 249.
[6] J. Banaś, V. Tomašić, A. Wesełucha-Birczyńska, M. Najbar, Catal. Today 119 (1–4) (2007) 199.
[7] P. Kornelak, B. Borzęcka-Prokop, L. Lityńska-Dobrzyńska, J. Wagner, D.S. Su, J. Camra, A. Wesełucha-Birczyńska, Catal. Today 119 (2007) 204.
[8] Y. Li, W.K. Hall, J. Catal. 129 (1991) 205.
[9] R.R. Sakaida, R.G. Rinker, Y.L. Wang, W.H. Corcoran, AIChEJ (1961) 658.
[10] A. Amirnazmi, J.E. Benson, M. Boudart, J. Catal. 30 (1973) 55.
[11] M. Iwamoto, S. Yokoo, K. Sakai, S. Kagawa, J. Chem. Soc., Faraday Trans. 1 (77) (1981) 1629.
[12] Y. Teraoka, T. Harada, H. Furukawa, S. Kagawa, in: L. Guczi, et al. (Eds.), New Frontiers in Catalysis, Elsevier, Amsterdam, 1993, p. 2649.
[13] M.C. Campa, V. Indovina, G. Mineli, G. Moretti, I. Pettiti, P. Porta, A. Riccio, Catal. Lett. 23 (1994) 141.
[14] M.A. Vannice, A.B. Walters, X. Zhang, J. Catal. 159 (1996) 119.
[15] M. Haneda, Y. Kintaichi, H. Hamada, Appl. Catal. E: Environ. 55 (2005) 169.
[16] J. Zhu, D. Xiao, J. Li, X. Yang, Y. Wu, J. Mol. Catal. A: Chem. 236 (2005) 182.
[17] M. Najbar, F. Mizukami, A. Białas, J. Camra, A. Wesełucha-Birczyńska, H. Izutsu, A. Góra, Top. Catal 11/12 (2000) 131.
[18] V. Tomašić, Z. Gomzi, S. Zrnčević, Appl. Catal. B: Environ. 18 (1998) 233.
[19] M. Najbar, J. Camra, A. Białas, A. Wesełucha-Birczyńska, B. Borzęcka-Prokop, L. Delevoye, J. Klinowski, Phys. Chem. Chem. Phys. 1 (1999) 4645.
[20] R. Roth, J. Waring, J. Res. NBS 70A (1966) 281.
[21] P. Kornelak, A. Michalak, M. Najbar, Catal. Today 101 (2005) 175.
[22] B. Modén, P. Da Costa, D.K. Lee, E. Iglesia, J. Phys. Chem. B 106 (37) (2002) 9633.
[23] B. Azambre, J. Banaś, M. Najbar, in press.